

# Observations of Cepheids with the *MOST* satellite: contrast between pulsation modes

N. R. Evans,<sup>1★</sup> R. Szabó,<sup>2</sup> A. Derekas,<sup>2,3</sup> L. Szabados,<sup>2,4</sup> C. Cameron,<sup>4</sup>  
J. M. Matthews,<sup>5</sup> D. Sasselov,<sup>1</sup> R. Kuschnig,<sup>5,6</sup> J. F. Rowe,<sup>7</sup> D. B. Guenther,<sup>8</sup>  
A. F. J. Moffat,<sup>9</sup> S. M. Rucinski<sup>10</sup> and W. W. Weiss<sup>6</sup>

<sup>1</sup>Harvard–Smithsonian Astrophysical Observatory, MS 4, 60 Garden St, Cambridge, MA 02138, USA

<sup>2</sup>Konkoly Observatory, Research Center for Astronomy & Earth Sciences, Konkoly Thege Miklós út 15-17, H-1121 Budapest, Hungary

<sup>3</sup>ELTE Gothard Astrophysical Observatory, H-9704 Szombathely, Szent Imre herceg út 112, Hungary

<sup>4</sup>Department of Mathematics, Physics & Geology, Cape Breton University, 1250 Grand Lake Road, Sydney, NS B1P 6L2, Canada

<sup>5</sup>Department of Physics and Astronomy, University of British Columbia, Vancouver, BC V6T1Z1, Canada

<sup>6</sup>University of Vienna, Institute for Astronomy, Türkenschanzstrasse 17, A-1180 Vienna, Austria

<sup>7</sup>NASA Ames Research Center, Moffett Field, CA 94035, USA

<sup>8</sup>Department of Astronomy and Physics, St Mary's University, Halifax, NS B3H 3C3, Canada

<sup>9</sup>Département de physique, Université de Montréal C.P. 6128, Succursale Centre-Ville, Montréal, QC H3C 3J7, Canada

<sup>10</sup>Department of Astronomy and Astrophysics, University of Toronto, 50 St George Street, Toronto, ON M5S 3H4, Canada

Accepted 2014 November 6. Received 2014 November 6; in original form 2014 July 30

## ABSTRACT

The quantity and quality of satellite photometric data strings is revealing details in Cepheid variation at very low levels. Specifically, we observed a Cepheid pulsating in the fundamental mode and one pulsating in the first overtone with the Canadian *MOST* (*Microvariability and Oscillations of Stars*) satellite. The 3.7-d period fundamental mode pulsator (RT Aur) has a light curve that repeats precisely, and can be modelled by a Fourier series very accurately. The overtone pulsator (SZ Tau, 3.1 d period) on the other hand shows light-curve variation from cycle to cycle which we characterize by the variations in the Fourier parameters. We present arguments that we are seeing instability in the pulsation cycle of the overtone pulsator, and that this is also a characteristic of the O – C curves of overtone pulsators. On the other hand, deviations from cycle to cycle as a function of pulsation phase follow a similar pattern in both stars, increasing after minimum radius. In summary, pulsation in the overtone pulsator is less stable than that of the fundamental mode pulsator at both long and short time-scales.

**Key words:** techniques: photometric – stars: individual: RT Aur – stars: individual: SZ Tau – stars: variables: Cepheids.

## 1 INTRODUCTION

Classical Cepheid variable stars have light and velocity variations which repeat very precisely. This is in contrast to variations from cycle to cycle sometimes seen in RR Lyrae stars (Szabó et al. 2010) and type II Cepheids (Sterken & Jaschek 1996). In fact it is the close repeatability in classical Cepheids which allows us to watch them evolve, that is to change their periods as they move through the instability strip in the HR diagram.

We have a few examples of changes in the light curves of Cepheids, partly due to new precision and long duration of observations. V473 Lyr (Burki et al. 1986) has a large change in amplitude over a period of about four years, resembling the Blazhko effect

(Molnar & Szabados 2014). Polaris itself has a variable amplitude which now begins to look cyclic, i.e. pulsation not evolution related (Arellano Ferro 1983; Bruntt et al. 2008). Extensive observations from the Wide Field Infrared Explorer (*WIRE*) satellite have helped to establish this behaviour in Polaris.

The field of view of the *Kepler* satellite contains numerous RR Lyr stars but only one classical Cepheid, V1154 Cyg. However, the extensive photometry of this star has produced an intriguing result (Derekas et al. 2012). Typical behaviour of the period variations is a change in the period of approximately 20 min which lasts for approximately 15 cycles, but then a return to the mean period. Results for classical Cepheids from the *CoRoT* satellite by Poretti are expected shortly.

Szabados (1983) has discussed period changes in Cepheids, both fundamental mode pulsators and overtone pulsators (low amplitude ‘s’ Cepheids). Based on his data, Evans, Sasselov & Short (2002)

★ E-mail: nevans@cfa.harvard.edu

have suggested that the rapid period change in Polaris (an overtone pulsator) is a characteristic of this group, a larger period instability than found in fundamental mode stars.

In order to follow up the discovery of a low level of period instability in the extensive *Kepler* data in V1154 Cyg and to further investigate differences in period instability between fundamental and overtone mode pulsators, we have obtained sequences of photometry with the *MOST* (*Microvariability and Oscillations of Stars*) satellite. The target stars were RT Aur (fundamental mode,  $P = 3.7$  d,  $\langle V \rangle = 5.5$  mag,  $V$  amplitude of 0.80 mag,<sup>1</sup> F8 Ib<sup>2</sup>) and SZ Tau (overtone mode,  $P = 3.1$  d,  $\langle V \rangle = 6.4$  mag,  $V$  amplitude of 0.33 mag F7 Ib). For comparison, V1154 Cyg is a fundamental mode pulsator with  $P = 4.9$  d and amplitude in  $V$  of 0.40 mag.

## 2 MOST OBSERVATIONS

The *MOST* satellite is a photometric satellite fully described in Walker et al. (2003), with the first science presented in Matthews et al. (2004).

For SZ Tau, observations were obtained in 2012 November (JD 245 6238–JD 245 6257) resulting in a continuous data set covering 19 d with a cadence of 1 min. For RT Aur, the observations were carried out in 2012 December 2012 (JD 245 6278–JD 245 6300). For this target, the 22 d-long observations were interleaved with another target, resulting in gaps in the light curve.

Data reduction was done following the standard steps outlined in Rowe et al. (2006a,b). Data can contain an artefact due to scattered earthshine in the *MOST* 101 min orbit, resulting in a signal with multiple peaks near 14 cycles d<sup>-1</sup>. The SZ Tau data were reprocessed beyond the standard processing to greatly reduce this signal. In RT Aur, the effect was not as prominent, but ultimately they were reprocessed also. Along with RT Aur a ‘comparison star’, HD 45237 was observed. This in principle would allow us to assess the quality of *MOST* photometry by comparing a relatively quiet star’s light variations to that of our Cepheids. HD 45237, which is a K0 IV 7th magnitude star, shows minor variations, totalling less than 0.01 mag. Specifically, it shows a low-amplitude, ‘Gaussian-shape’ brightening event in the middle of our observing session lasting for 6 d. Other than that, the frequency spectrum of the star nicely shows the alias frequencies due to the sampling around 14 c d<sup>-1</sup>. We did not use this star further in our analysis.

## 3 LIGHT-CURVE ANALYSIS

A difference between the light curves of RT Aur and SZ Tau is immediately obvious from the first plots of the light curves. Fig. 1 shows the data of RT Aur phased by a period of 3.7348 d and SZ Tau phased by a period of 3.149 407 d, respectively. The RT Aur light curve repeats very precisely, notably at maximum light. On the other hand, SZ Tau shows tight sequences at maximum for each cycle which, however, vary in brightness from cycle to cycle. Similar but less pronounced behaviour is seen at minimum light.

The next step is to investigate the departures of the data from a strict cycle-to-cycle repetition. In Fig. 1, we plot the consecutive pulsational cycles with different symbols and colours. This figure shows that while the pulsational cycles of RT Aur repeat regularly, there is a considerable deviation in the light variation of SZ Tau, especially around and before the brightness maximum.

The rest of this discussion will be to quantify the contrasting behaviour between the fundamental and the overtone pulsators.

The first step in the analysis is to fit a Fourier polynomial to the data:

$$m = A_0 + \sum_{i=1}^N A_i \times \sin(2\pi i f t + \Phi_i), \quad (1)$$

where  $m$  is the magnitude,  $A$  is the amplitude,  $f$  is the frequency,  $t$  is the time of observation,  $\Phi_i$  is the phase and  $i$  runs from 1 to  $N$ , where  $N$  is 9 and 10 for SZ Tau and RT Aur, respectively. The sequence in  $N$  was stopped when there were only many low frequency peaks left. Tables 1 and 2 list the result of our Fourier analysis performed by using PERIOD04 (Lenz & Breger, 2005), i.e. frequencies, amplitudes, and phases and their errors for RT Aur and SZ Tau. Frequencies identified as harmonics of the fundamental oscillation are indicated in the first column. Other frequencies found in the analysis are listed in the tables (in the order of increasing frequency) but are not included in further analysis.

Figs 2 and 3 show the Fourier spectra of RT Aur and SZ Tau, respectively. In the left and centre panels of Fig. 2, the Fourier spectrum of RT Aur is shown (left) and then again pre-whitened by the 10 harmonics in Table 1 (centre). A residual orbital signal near 14 c d<sup>-1</sup> is apparent in similar figures which extend out to that frequency because the target was interleaved with another target. The pre-whitened spectrum (Fig. 2 centre) shows that the removal of the main frequency and its harmonics reduces the signal from the star to noise. The right-hand panel of Fig. 2 is the window function for RT Aur. Fig. 3 provides the Fourier spectrum for SZ Tau. The pre-whitened spectrum (Fig. 3 centre) with the harmonics of the pulsational frequency in Table 1 removed, however, leaves a complicated pattern of frequencies. This contrasts to the reduction to a noise spectrum in the pre-whitened RT Aur spectrum (Fig. 2 centre).

The noise level and  $\sigma$  were estimated from a quiet portion of the Fourier spectrum (Figs 2 and 3 centre). By noise in RT Aur’s Fourier spectrum, we mean the average of the residuals after removing  $f_0$  and its harmonics, which we find featureless. Values of  $\sigma$  in Tables 1 and 2 are the uncertainty of a given fitted parameter determined with the Monte Carlo simulation performed using PERIOD04. For RT Aur and SZ Tau they are noise:  $1.3 \times 10^{-4}$  and  $4.9 \times 10^{-5}$ , respectively. The S/N in Tables 1 and 2 was generated using these values.

### 3.1 Comparison of SZ Tau and RT Aur

The RT Aur data are well represented by Fourier series for a single frequency and its harmonics and the pattern due to the orbit of the satellite. The SZ Tau data, on the other hand, have deviations from the Fourier fit.

#### 3.1.1 Light-curve stability

In Section 3, we showed that the fundamental pulsator RT Aur has the expected behaviour for a Cepheid. While there is some scatter for the moments of maximum brightness, the median brightness on the ascending branch repeats in a strictly regular manner. (Median brightness is the average value of the adjacent minimum and maximum, which is not identical to the mean magnitude calculated for the complete pulsational cycle). The other *MOST* Cepheid, SZ Tauri (overtone pulsator) shows perceptible cycle-to-cycle changes. In this section, we will consider how this contrasting stability of the light curves of a fundamental mode

<sup>1</sup> <http://www.astro.utoronto.ca/DDO/research/cepheids/>

<sup>2</sup> <http://simbad.u-strasbg.fr/simbad/>

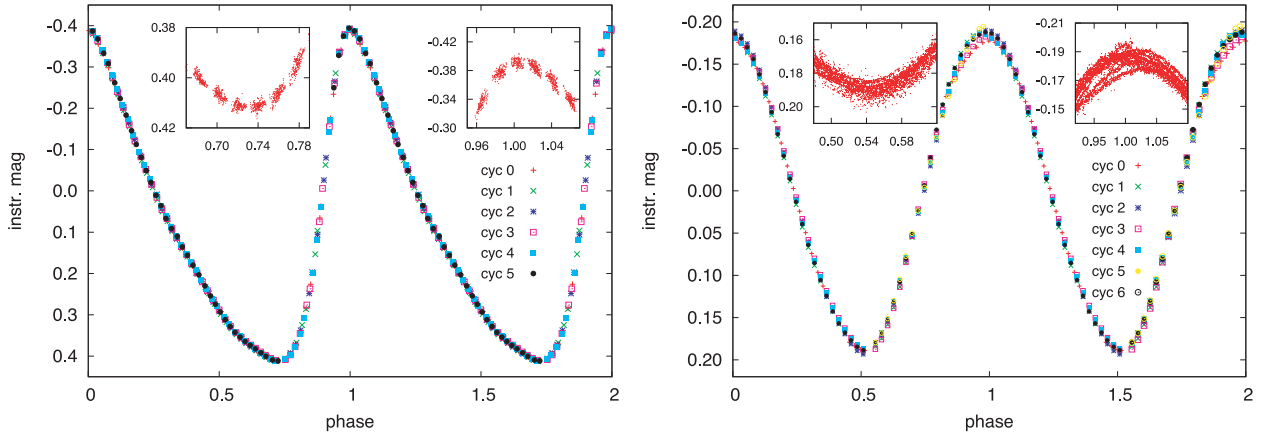


**Figure 1.** *MOST* light curves of two Cepheids phased by pulsation period: the fundamental mode pulsator RT Aur (left-hand panel) and SZ Tau (right-hand panel) which pulsates in the first overtone. Note the different scale on the y-axis. The insets show blow-ups of the maxima and minima indicated by the rectangles. The data have been binned with a 0.075 d bin size. A comparison of the two panels clearly shows that the pulsational cycles of RT Aur repeat regularly, while there is a substantial deviation in the light variation of SZ Tau, especially around and before the pulsational maximum.

**Table 1.** Frequencies, amplitudes and phases of the identified frequency peaks in the frequency spectrum of RT Aur.

ID	Frequency ( $\sigma$ ) ( $d^{-1}$ )	Amplitude ( $\sigma$ ) (mag)	Phase ( $\sigma$ ) (rad)	S/N
$f_0$	0.268 19 (0.000 01)	0.346 90 (0.000 09)	0.409 47 (0.000 04)	4954
$2f_0$	0.536 39 (0.000 02)	0.128 95 (0.000 09)	0.236 72 (0.000 11)	1840
$3f_0$	0.804 58 (0.000 04)	0.055 76 (0.000 09)	0.063 97 (0.000 24)	795
$4f_0$	1.072 77 (0.000 09)	0.025 15 (0.000 09)	0.921 08 (0.000 53)	357
$5f_0$	1.340 97 (0.000 20)	0.010 98 (0.000 09)	0.720 03 (0.001 23)	155
$6f_0$	1.609 16 (0.000 37)	0.005 82 (0.000 09)	0.547 19 (0.002 30)	81
$7f_0$	1.877 36 (0.000 75)	0.002 93 (0.000 09)	0.374 58 (0.004 72)	40
$8f_0$	2.145 55 (0.001 47)	0.001 49 (0.000 09)	0.165 64 (0.009 17)	19
$9f_0$	2.413 74 (0.002 48)	0.000 78 (0.000 09)	0.009 67 (0.015 46)	9
$10f_0$	2.681 94 (0.003 44)	0.000 55 (0.000 09)	0.819 81 (0.021 65)	6
	0.037 66 (0.008 69)	0.001 13 (0.006 19)	0.525 39 (0.008 39)	14
	0.085 29 (0.009 90)	0.001 03 (0.005 05)	0.682 28 (0.008 28)	13
	0.182 32 (0.002 10)	0.000 88 (0.000 09)	0.630 75 (0.011 42)	11

**Table 2.** Frequencies, amplitudes and phases of the identified frequency peaks in the frequency spectrum of SZ Tau.

ID	Frequency ( $\sigma$ ) ( $d^{-1}$ )	Amplitude ( $\sigma$ ) (mag)	Phase ( $\sigma$ ) (rad)	S/N
$f_0$	0.317 52 (0.000 01)	0.188 00 (0.000 01)	0.440 34 (0.000 02)	6526
$2f_0$	0.633 07 (0.000 10)	0.008 11 (0.000 02)	0.617 23 (0.000 41)	280
$3f_0$	0.954 63 (0.000 23)	0.003 74 (0.000 02)	0.717 00 (0.000 92)	128
$4f_0$	1.272 59 (0.000 57)	0.001 30 (0.000 02)	0.000 12 (0.002 50)	43
$5f_0$	1.595 86 (0.000 77)	0.000 77 (0.000 02)	0.956 22 (0.004 16)	25
$6f_0$	1.910 50 (0.000 92)	0.000 62 (0.000 02)	0.393 91 (0.005 01)	20
$7f_0$	2.223 25 (0.000 97)	0.000 59 (0.000 02)	0.507 97 (0.004 66)	19
$8f_0$	2.546 86 (0.001 03)	0.000 54 (0.000 02)	0.946 17 (0.005 73)	17
$9f_0$	2.867 53 (0.001 46)	0.000 38 (0.000 02)	0.155 96 (0.008 12)	11
	0.046 69 (0.000 66)	0.001 25 (0.000 02)	0.939 45 (0.003 09)	42
	0.184 31 (0.001 93)	0.000 74 (0.000 03)	0.610 63 (0.004 41)	24
	0.246 63 (0.000 50)	0.002 75 (0.000 03)	0.535 42 (0.001 22)	94
	0.495 02 (0.000 60)	0.001 68 (0.000 02)	0.926 75 (0.002 88)	57
	0.541 26 (0.000 43)	0.002 43 (0.000 02)	0.749 11 (0.001 92)	83
	1.070 39 (0.003 30)	0.001 13 (0.000 14)	0.443 14 (0.006 79)	38
	1.111 49 (0.004 26)	0.000 87 (0.000 10)	0.790 06 (0.041 08)	29
	1.148 50 (0.003 23)	0.000 99 (0.000 11)	0.019 84 (0.101 69)	33
	1.392 26 (0.000 74)	0.000 88 (0.000 02)	0.762 67 (0.003 61)	29

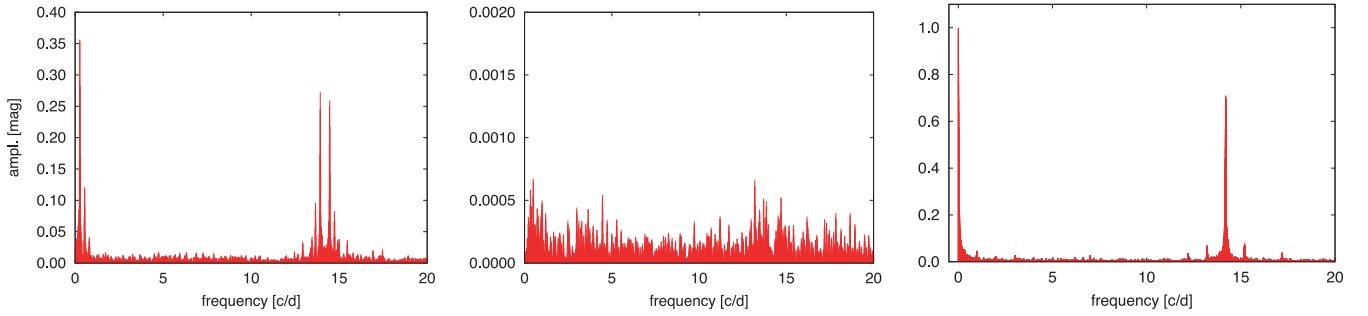


**Figure 2.** Fourier spectrum of RT Aur (left-hand panel); the same, but pre-whitened by the 10 frequencies in Table 1 (the pulsational frequency and its harmonics) (middle panel); spectral window of the RT Aur observations of *MOST* (right-hand panel). The feature near  $14 \text{ c d}^{-1}$  is due to interleaving the observations with another target.

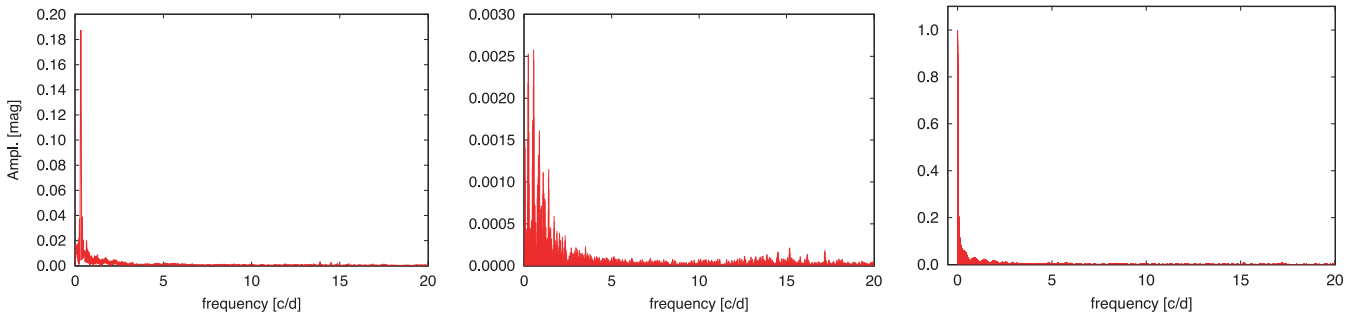


**Figure 3.** Fourier spectrum of SZ Tau (left-hand panel); the same, but pre-whitened by the 9 frequencies in Table 2 (the pulsational frequency and its harmonics) (middle panel); spectral window of the SZ Tau observations of *MOST* (right-hand panel).

and an overtone mode pulsator is manifested in the Fourier parameters. For this, we fitted a high-order Fourier polynomial at the primary frequency and its harmonics using equation (1) for each cycle. Then, we characterized the light-curve shapes with the Fourier parameters (Simon & Teays 1982), and show results for  $R_{21} = A_2/A_1$ ,  $R_{31} = A_3/A_1$  and  $R_{51} = A_5/A_1$  as well as  $\phi_{21} = \phi_2 - 2\phi_1$  and  $\phi_{31} = \phi_3 - 3\phi_1$ .

The top-left panel of Fig. 4 shows the amplitude  $A_1$  of RT Aur for the six cycles covered. The arrows in each panel show the approximate range of variation between cycles, together with the percentage of variation. Note that the variation in this amplitude is only about 0.9 per cent between the cycles. In SZ Tau (top-right panel in Fig. 4), the variation in the Fourier amplitude  $A_1$  is 3.6 per cent. Similarly, the variation of the amplitudes  $R_{21}$ ,  $R_{31}$ , and  $R_{51}$  is shown in Fig. 4 for RT Aur (lower-left panels) and for SZ Tau (lower-right panels). For RT Aur  $R_{21}$ ,  $R_{31}$ , and  $R_{51}$  vary by approximately 1.5, 3.2, and 9.2 per cent, respectively. For SZ Tau, the respective variations are closer to 50, 100, and 120 per cent. Similarly, the variations in phase parameters  $\phi_{21}$  and  $\phi_{31}$  are modest in RT Aur (left-hand panels in Fig. 5) but much larger in SZ Tau (right-hand panels in Fig. 5).

In summary, all the light-curve quantities are much more variable in SZ Tau than in RT Aur. We can also compare the variations in RT Aur with those of the fundamental mode Cepheid in the *Kepler* field (V1154 Cyg), which has a much longer series of observations (Derekas et al. 2012). The  $A_1$  amplitude for V1154 Cyg has comparably small variations over the intervals that correspond to the length of the *MOST* observations. However, on time-scales as long as a year it has larger amplitude variations. Thus there may be larger variations than we have seen in the *MOST* RT Aur data, but it is on a much longer time-scale. Other Fourier parameters in V1154 Cyg have variations comparable to those of RT Aur.

### 3.1.2 Phase dependence

To further study the deviations from the Fourier representation of SZ Tau, Fig. 6 (right) shows the deviations from the 9-term representation. The high quality of the data allows us to inspect individual cycles of the two stars. As a comparison, the left-hand panel of Fig. 6 features the much smaller residuals of RT Aur. These small residuals show clear pattern however. They almost vanish around minimum light, and are larger in other pulsational phases. For SZ Tau, there are some differences in the residuals from cycle to cycle (Fig. 6 top right). However, the deviations have a reasonably consistent pattern, including sharp inflections following minimum radius (Fig. 6, top right). When the standard deviations between cycles are created as a function of phase (Fig. 6 bottom), the phase dependence is surprisingly similar for RT Aur (left) and SZ Tau (right). That is both the fundamental and overtone pulsators show an increased standard deviation around minimum radius when the next pulsation cycle is initiated by a ‘shove’ from the pulsation piston. After maximum radius, the ‘coasting phase’ the deviations between cycles decrease, and remain small until the ‘shove’ from the next cycle.

## 4 O – C DIAGRAMS

To put the *MOST* observations into the long-term context, Fig. 7 shows the O – C diagrams of both stars and Fig. 8 shows the O – C diagrams from the *MOST* observations.

### 4.1 RT Aur

For RT Aur, several studies of the variations in the pulsation period are available in the literature, of which the latest are: Szabados (1991), Berdnikov, Mattei & Beck (2003), Meyer (2004), and Turner

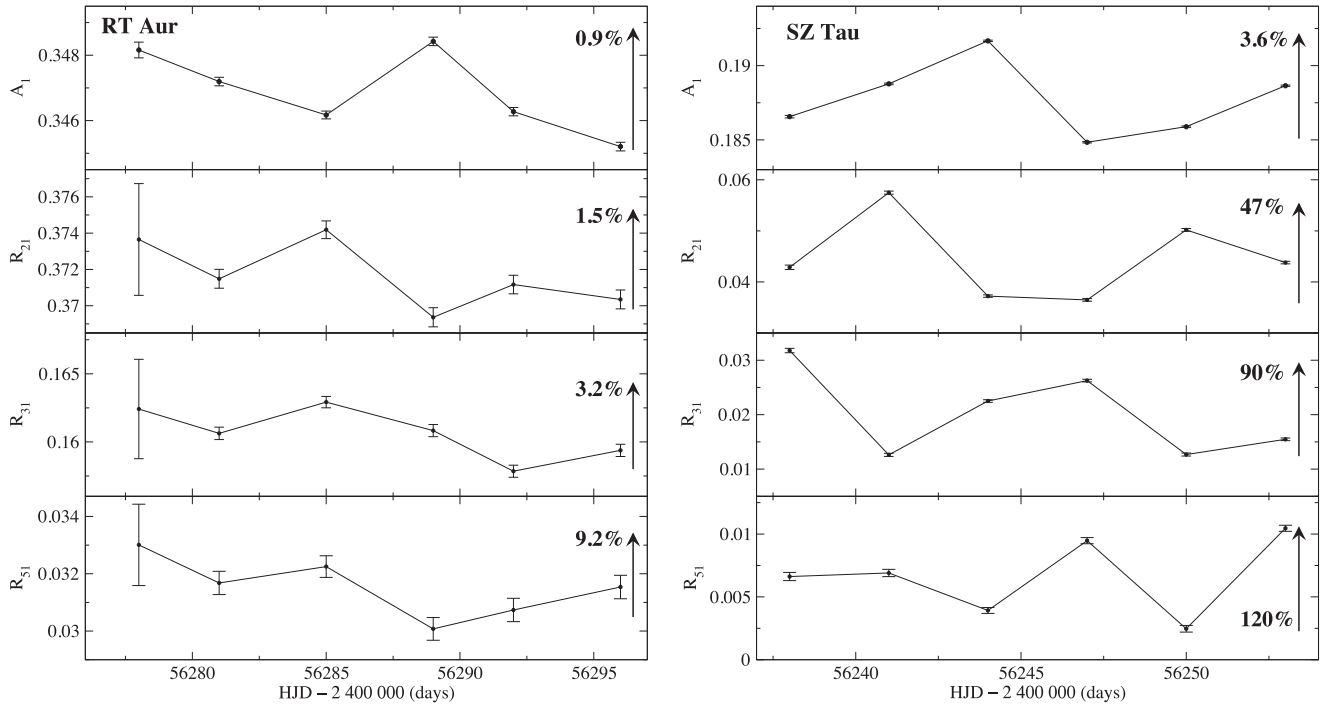


**Figure 4.** Fourier parameters of RT Aur (left-hand panels) and SZ Tau (right-hand panels) from the *MOST* observations. The arrows on the right-hand side of each panel show the approximate variation of the parameters during the cycles observed; the percentage of variation is given by each arrow. Top panels: variation of the  $A_1$  amplitude between cycles. The panels below show the variation of the amplitude ratios  $R_{21}$ ,  $R_{31}$ , and  $R_{51}$ . The errors in the first cycle of RT Aur are unusually large because the cycle was incompletely covered.

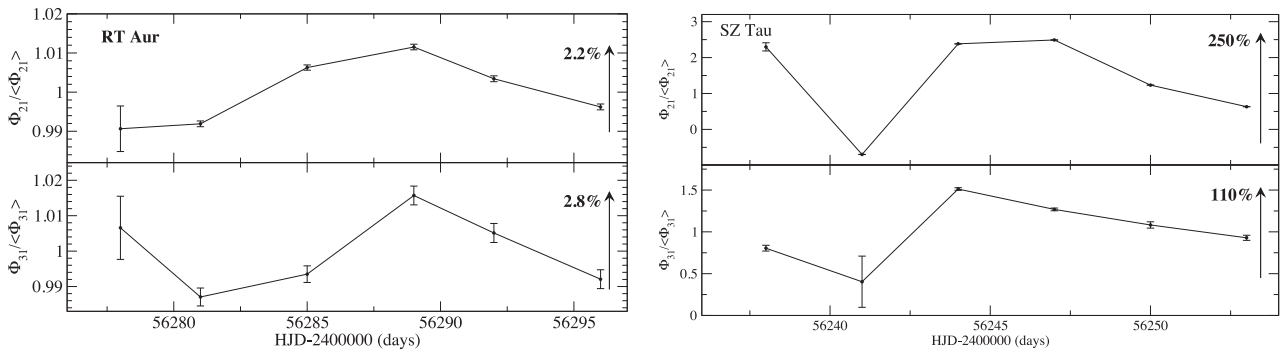


**Figure 5.** Fourier parameters of RT Aur (left-hand panels) and SZ Tau (right-hand panels) from the *MOST* observations. Again, the arrows indicate the approximate variation between cycles. Top panels: the variation of  $\phi_{21}/\langle\phi_{21}\rangle$ . Bottom panels: variation of  $\phi_{31}/\langle\phi_{31}\rangle$ . The errors in the first cycle of RT Aur are unusually large because the cycle was incompletely covered.

et al. (2007). The O – C diagram based on the normal brightness maxima published by Turner et al. (2007) is shown in the left-hand panel of Fig. 7. Their tables 2 and 3 are used, but data with an assigned weight less than 1 have been omitted and several values based on photometric data which they omitted are included, as well as the new *MOST* data. The new set of normal maxima together with references is listed in Table 3, which is available in the electronic version. In that table the O – C residuals correspond to the updated ephemeris:

$$C_{\max} = 2441\,723.7678 + 3.728\,255 \times E \pm 0.0077 \pm 0.000\,003. \quad (2)$$

This ephemeris was obtained by a weighted linear least-squares method based on the tabulated normal maxima. A weight of 1, 2, or

3 has been assigned to the individual data series depending on the number and quality of the data points. For a better visualization, we only plotted the most reliable O – C residuals (those with weights 2 or 3) in the left-hand panel of Fig. 7. Part of the scatter may be due to the uncertainty in the determination of the moments of individual normal maxima. However, another cause is also present. The 0.05 d difference within three weeks between the O – C values for the brightness maxima (denoted as open circles in the left-hand panel of Fig. 8) from the accurate and uninterrupted *MOST* data is intrinsic to stellar pulsation. It is also seen, however, that the pulsation period of RT Aur is very stable for the moments of the median brightness on the ascending branch of the light curve (filled circles in the left-hand panel of Fig. 8). This means that the fluctuation in the O – C values is caused by the slight variability in the shape of the light curve. In fact, the 0.05 d fluctuation in the *MOST* O – C values

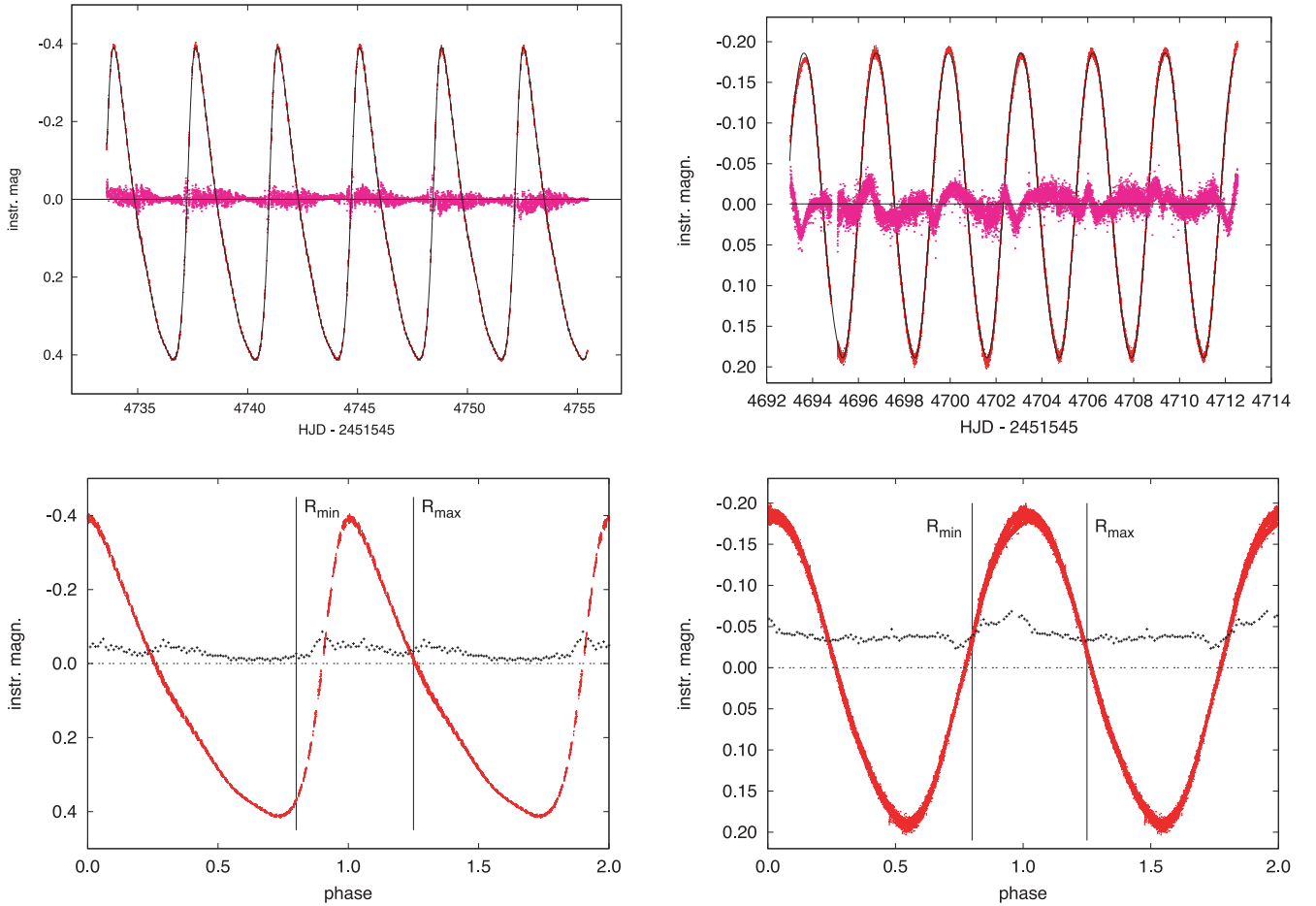


**Figure 6.** The fit of the light curve of RT Aur (top-left panel) and SZ Tau (top-right panel). Red points: observations, black curve: Fourier fit, magenta points: residuals magnified three times to enhance visibility. Residuals were created from a 10-term Fourier fit of RT Aur from Table 1 (left-hand panel) and for SZ Tau from a 9-term Fourier fit taken from Table 2 (right-hand panel). Bottom: standard deviations between cycles as a function of phase binned into 100 phase bins. Left: RT Aur – the phased light curve (red) is compared with the standard deviations between cycles, magnified by three times for plotting (black dots). Maximum and minimum radii are also shown. Right: the same for SZ Tau.

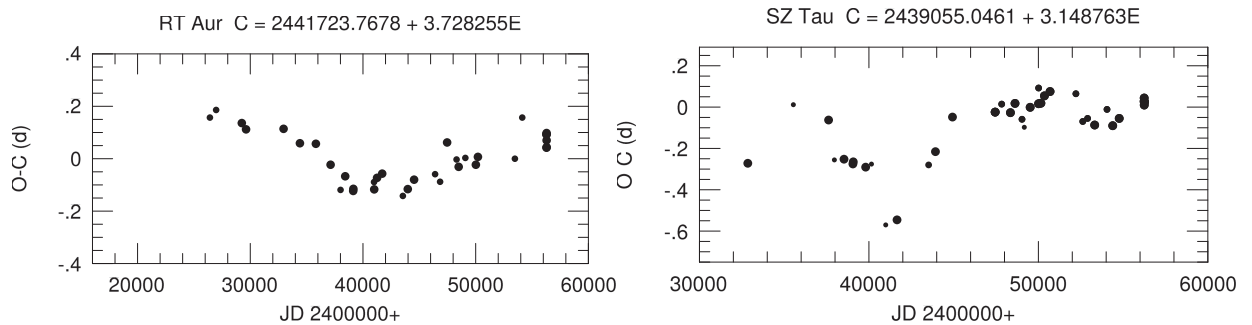


**Figure 7.** Long-term  $O - C$  variations of RT Aur (left-hand panel) and SZ Tau (right-hand panel) with the epoch and period used. While both stars show significant variations, RT Aur seems to change its pulsational period more smoothly than SZ Tau. Symbol sizes correspond to the weight assigned to the  $O - C$  value listed in Tables 7 and 8.

corresponds to 1.3 per cent of the pulsation period which is quite compatible with the fluctuations of the Fourier amplitude and phase parameters visualized in the left-hand panel of Fig. 6.

In RT Aur the  $O - C$  diagram (period change; left-hand panel of Fig. 7) has relatively smooth variation. If the pattern of the  $O - C$  residuals is approximated by a positive parabola, then the rate of period increase is  $0.000\,986\text{ d century}^{-1}$ . The pattern of the  $O - C$  residuals of RT Aur has been interpreted in different ways,

from a simple parabola (Ferne 1993) to a more complicated form (Turner et al. 2007). The amplitude from the  $O - C$  variations, however, is commensurate with an evolutionary time-scale, and as noted by Ferne, is much smaller than that of the first overtone pulsator Polaris. Turner et al. interpret a wave-like structure to the  $O - C$  residuals as light-time effect in a very long-period orbit ( $26\,429\text{ d} = 72\text{ yr}$ ); however, they find this difficult to reconcile with the constraints on the companion. We present a summary of

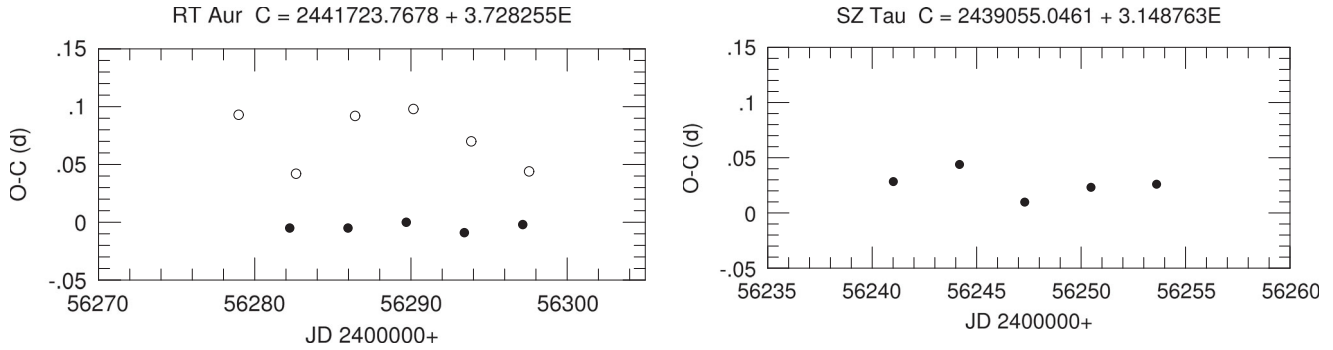


**Figure 8.** Left:  $O - C$  variations of RT Aur based on the *MOST* observations. Open circles refer to moments of brightness maxima, filled circles represent  $O - C$  values for moments of the median brightness on the ascending branch (offset by 0.360 d to facilitate a direct comparison with those for light maxima) Right:  $O - C$  variations of SZ Tau based on the *MOST* observations.

**Table 3.**  $O - C$  values of RT Aurigae.  $E$  is the epoch of the determination in cycles;  $W$  is the weight. This is only a portion of the full version available online only.

$JD_{\odot}$	$E$	$O - C$	$W$	Data source
240 0000		(d)		
209 57.478	-5570	0.091	1	Turner et al. (2007)
227 84.241	-5080	0.009	1	Turner et al. (2007)
264 19.438	-4105	0.157	2	Turner et al. (2007)
269 71.249	-3957	0.186	2	Turner et al. (2007)
275 04.400	-3814	0.197	1	Turner et al. (2007)

**Table 4.**  $\gamma$ -velocities of RT Aurigae.

JD	$v_{\gamma}$	$\sigma$	Data source
240 0000	( $\text{km s}^{-1}$ )	( $\text{km s}^{-1}$ )	
182 30	21.0	0.5	Petrie (1932) (obs.: Duncan)
212 10	19.9	2.0	Kiess (1917)
248 00	21.0	0.5	Petrie (1932)
409 79	19.8	1.0	Evans (1976)
434 49	19.2	1.5	Wilson et al. (1989)
434 57	19.7	1.0	Beavers & Eitter (1986)
439 62	18.0	2.0	Barnes, Moffett & Slovak (1987)
457 17	20.0	1.0	Gieren (1985)
468 66	19.7	1.5	Gorunya et al. (1996)
486 00	19.3	0.5	Gorunya et al. (1996)
501 00	20.0	0.5	Gorunya et al. (1996)
503 50	20.0	0.8	Kiss (1998)
551 10	18.5	0.5	Takeda et al. (2013)

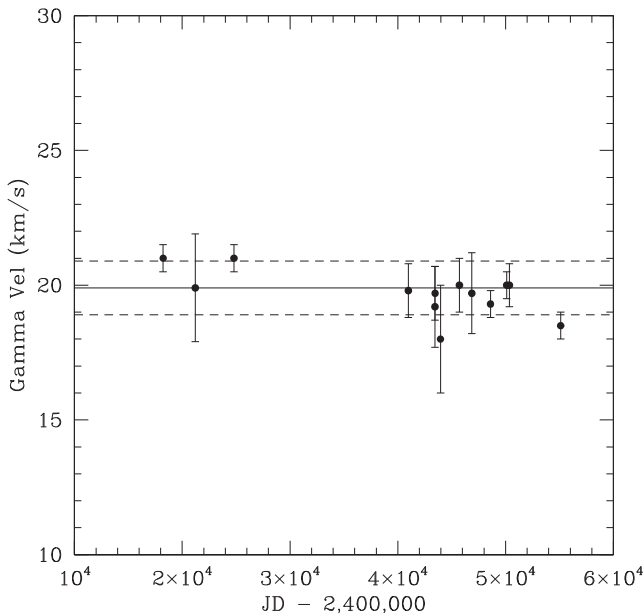


**Figure 9.** Variations of the  $\gamma$  (systemic) velocity of RT Aur. The solid line is the mean; dashed lines indicate  $\pm 1 \text{ km s}^{-1}$  from the mean. None of the velocities deviate from the  $\pm 1 \text{ km s}^{-1}$  band by more than  $1\sigma$ .

the systemic ( $\gamma$ ) velocity data in Fig. 9 and Table 4 including the most recent data from Takeda et al. (2013). None of the systemic velocities differs from a band of  $\pm 1 \text{ km s}^{-1}$  around the mean value by more than  $1\sigma$ , making it unlikely that orbital motion has been detected, although a tendency of a slight decrease in the  $\gamma$ -velocity values is noticeable. Further observations are necessary to clarify the question of binarity of RT Aur.

## 4.2 SZ Tau

SZ Tau, on the other hand, has more erratic variations in its  $O - C$  diagram, and in particular, times when the  $O - C$  is increasing alternating with periods when it is decreasing. That is, periods are neither monotonically increasing nor decreasing as expected for evolution through the instability strip.  $O - C$  diagrams showing the variability of the pulsation period for many stars are available in Szabados (1977, 1991) and Berdnikov & Pastukhova (1995). These latter authors approximated the  $O - C$  graph of SZ Tau with a parabola implying a continuous period decrease with erratic changes superimposed. According to Szabados (1977, 1991), however, the linear sections in the  $O - C$  graph imply that there are preferred values of the period to which the Cepheid returns during its pulsation on a time-scale of several years to decades. The  $O - C$  residuals based on previous photoelectric and CCD observations are plotted in the right-hand panel of Fig. 7, extending the time base by two decades as compared with the latest one by Berdnikov & Pastukhova (1995).

The  $O - C$  residuals based on all available accurate (photoelectric or CCD) measurements are listed in Table 5 together with the references in the electronic version. For low-amplitude Cepheids, such as SZ Tau, the preferred light-curve feature for  $O - C$  studies is not the moment of the light maximum because of the large uncertainty in determining the phase of the brightness extremum during the shallow variation. Instead, the behaviour of the pulsation period can be followed by studying the moment of the median brightness on the ascending branch of the light curve, where the variations

**Table 5.** O – C values of SZ Tauri. This is only a portion of the full version available online only.

JD <sub>⊙</sub> 240 0000 +	<i>E</i>	O – C (d)	<i>W</i>	Data source
328 51.7111	–1970	–0.2719	3	Eggen (1951)
355 41.0382	–1116	0.0116	1	Walraven, Muller & Oosterhoff (1958)
376 19.1476	–456	–0.0626	3	Mitchell et al. (1964)
379 62.1697	–347	–0.2556	1	Williams (1966)
385 28.9506	–167	–0.2521	3	Wisniewski & Johnson (1968)

**Table 6.** New *UBV* photometric data of SZ Tauri. This is only a portion of the full version available online only.

JD <sub>⊙</sub> 240 0000 +	<i>V</i> (mag)	<i>B</i> – <i>V</i> (mag)	<i>U</i> – <i>B</i> (mag)
485 93.5264	6.385	0.739	0.526
485 94.5173	6.616	0.874	0.612
486 46.3869	6.488	0.779	0.528
486 47.3421	6.431	0.758	0.562
490 32.3006	6.670	0.875	0.615

in the brightness are the steepest during the pulsational cycle (see section 2.2 in Derekas et al. 2012). The residuals are determined from the *V*-band light curves (or the nearest band to it), and refer to the moments of median brightness on the ascending branch corresponding to the ephemeris:

$$C_{\text{med}} = 2439\,055.0461 + 3.148\,763 \times E \pm 0.0283 \pm 0.000\,006. \quad (3)$$

A least-squares linear fit has been applied to the O – C residuals after  $E = 2666 = \text{HJD } 2447450$  that resulted in equation (3). The resulting O – C diagram is plotted in the right-hand panel of Fig. 7. Table 5 contains some O – C residuals based on photoelectric *UBV* observations obtained with the photometer attached to the 50 cm Cassegrain telescope at the Pizskéstető Mountain Station of the Konkoly Observatory between 1991 and 2003. The individual photometric data are listed in Table 6 (observer: L. Szabados). The full table is provided in the electronic version.

The scatter of the plot for the last decades where the pulsation period was approximated as a constant value of 3.148 763 d exceeds the observational uncertainty, and this is the case for the O – C residuals derived from the *MOST* data, as well. Cycle-to-cycle period change is present in the right-hand panel of Fig. 8, similar to V1154 Cyg. The period in individual cycles varies within 0.7 per cent of the average value of the pulsation period. On a longer time-scale, there are erratic cycle-to-cycle variations (right-hand panel of Fig. 7).

### 4.3 Pulsation mode

The erratic cycle-to-cycle variation of SZ Tau (as compared with RT Aur) is characteristic of overtone pulsators (e.g. fig. 2 in Berdnikov et al. 1997). In the past shorter data strings have been fitted to parabolas implying to rapid period changes (see Szabados 1983) but more extensive data appear to suggest that for many overtone pulsators the period variations are more complicated than simple monotonic changes.

The rigorous interpretation of O – C diagrams has been discussed extensively by Koen (2006), based on the combination of measurement error, a long-term change in period, and random changes in the

period. Specifically, he demonstrates that it is possible for random changes in the period to mimic long-term changes in the period. Full analysis of the O – C period changes in Fig. 7 is beyond the scope of this paper, but we will put the O – C characteristics of the overtone (SZ Tau) in context, and discuss instances where the O – C diagram is consistent with a Koen dominant long-term variation, and where it is consistent with a Koen dominant random period jitter.

In this section, we develop a qualitative summary of period variation in overtone Cepheids based on the O – C curves of Berdnikov et al. (1997) of low-amplitude Cepheids. The first step is to confirm the pulsation mode. For this we have used primarily the classifications of Groenewegen & Oudmaijer (2000), Kienzle et al. (1999), and Sachkov (1997). The pulsation mode of V1334 Cyg was discussed by Evans (2000) and the pulsation mode of V473 Lyr by Burki et al. (1986). FF Aql was found not to be an overtone pulsator by Benedict et al. (2007). In three cases, (GI Car, V532 Cyg, and VZ CMa) the star was classified as an overtone pulsator by Kienzle et al. but not Groenewegen & Oudmaijer. We have retained the overtone designation since the sensitivity to pulsation mode varies depending on both the period ranges and the diagnostic itself.

We then have used the O – C diagrams of Berdnikov et al., and identified three categories of period change. First, seven stars (EU Tau,  $\alpha$  UMi, SU Cas, GI Car, V1726 Cyg, V473 Lyr [second overtone pulsator], and UY Mon) were found to have O – C diagrams consistent with a parabolic fit (figs 1 and 2 in Berdnikov et al.) all indicating increasing period (discussed below). Only EU Tau and  $\alpha$  UMi, however, have O – C diagrams which were unquestionably parabolic fits, showing period variation which is particularly rapid. These are consistent with the Koen class of long-term period variation.

In the second group, seven other stars (BY Cas, V379 Cas, DT Cyg, V532 Cyg, DX Gem, EV Sct, and SZ Tau; figs 3 and 4 in Berdnikov et al.) clearly have variations in their O – C diagrams, but the variations switched from between positive and negative and back in an apparently cyclic way. SZ Tau (right-hand panel of Fig. 7) exhibits this behaviour. This ‘activity’ in the period is clearly not caused by monotonic evolution through the instability strip, and suggest a that Koen period jitter is dominant. The excursions around a mean period suggest a pulsation related cause rather than a secular change due to evolution.

There is a third group of 15 stars (VZ CMa, GH Car, V419 Cen, BG Cru, V1334 Cyg, V526 Mon, QZ Nor, V440 Per, EK Pup, MY Pup, V335 Pup, V950 Sco, AH Vel, FZ Car, and AZ Cen; fig. 5 in Berdnikov et al.) which have no pattern in the photometric O – C residuals. This may be because the data series are not long enough, or the values are not accurate enough or in many cases the gaps between the times of observation obscure any correlation. It is likely that at least some of these have period jitter, possibly at a lower level and over a longer time-scale than the more prominent fluctuations in the first two groups.

In summary, the photometric monitoring of these 29 overtone pulsators shows that nearly half of them have period variation. This includes the second group showing substantial period jitter. Thus on the scale of decades there is evidence of considerable period variation in overtone pulsators, including both the Koen categories of long-term change and random period jitter.

## 5 DISCUSSION

The *MOST* observations display two characteristics of pulsation not seen before in less plentiful and less accurate data. First, the light curves as exhibited by the Fourier parameters are more variable in the overtone pulsator SZ Tau than in the fundamental mode pulsator RT Aur. On the other hand, the differences between cycles display a similar pattern as a function of phase (Fig. 6). We have made preliminary explorations for explanations as discussed in the sections below.

### 5.1 Mode dependence

The intensive observations of RT Aur and SZ Tau with the *MOST* satellite have demonstrated that the overtone pulsator (SZ Tau) has more instability in its pulsation cycle than the fundamental mode Cepheid (RT Aur). This is apparent in simple repetition of the light curve from cycle to cycle (Figs 1 and 2), the Fourier spectrum of the observations (Figs 3 and 4), the Fourier parameters cycle by cycle (Figs 5 and 6) and the O – C diagrams (Figs 8 and 9). As a preliminary consideration, we note that the node of a first overtone pulsator occurs higher in the envelope than that of a fundamental mode pulsator. This may create differences in the pulsation even for stars of reasonably similar period, mass, and temperature.

### 5.2 Effect of turbulent convection

The quality and quantity of *MOST* and *Kepler* satellite observations have revealed changes in the periods and light curves of SZ Tau and V1154 Cyg. Explanations due to evolution, mass-loss, and binary light-time effect are not adequate for the non-monotonic variations as discussed in Section 5.3. It is suggested that there is an instability in the pulsation itself which is responsible.

In order to check whether turbulent convection in the partial ionization zones can cause cycle-to-cycle light-curve variations, we computed models with the Florida–Budapest code (Kolláth et al. 2002). We used similar parameters and settings as Szabó, Buchler & Bartee (2007). To study SZ Tau, we computed an overtone pulsator model, with a mass of  $5.25 M_{\odot}$ ,  $L = 1979 L_{\odot}$  and  $T_{\text{eff}} = 6075$  K and solar metallicity. The model has a linear overtone period of 3.106 d.

Figs 10(a) and 10(b) show the variation of the bolometric luminosity and the radii of the topmost layers of the model after reaching its limit cycle corresponding to the radial first overtone mode, respectively. In panel (c), we plot the turbulent energy as a function of time and zone number (from 78 to 121). The magnitude of the turbulent energy is colour coded. This range of zones captures the hydrogen ionization zone featuring the strongest turbulent energy throughout the pulsational cycle, of the order of  $10^{10}$ – $10^{12}$  erg per zone. The energy is highest where the *MOST* light curve of SZ Tau shows the largest scatter.

However, the magnitude of the turbulent energy content is negligible compared to the kinetic energy due to the pulsation as is shown in Fig. 10(d). Here, we show the logarithm of the ratio of the turbulent and kinetic energy for each zone as a function of time.

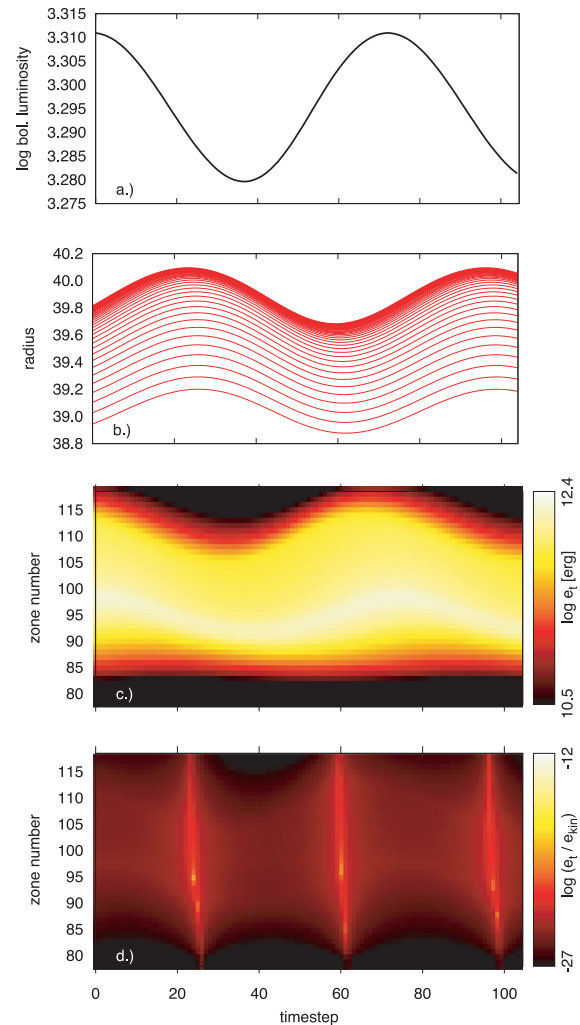


**Figure 10.** (a) Bolometric luminosity variation of our model overtone Cepheid; (b) radius variation of upper zones in the model; (c) turbulent energy as a function of time and zone number; (d) logarithm of the ratio of the turbulent and kinetic energy for each zone as a function of time. Maximum values are reached when local velocity approaches its minima.

The largest values are attained for the local velocity minima (for a given mass zone), which is the dominant term in this quantity. The discrepancy is huge, the turbulent energy is 10–20 orders of magnitude less than the kinetic energy. Even if the total turbulent energy could be converted to kinetic energy the modulation of the light curve would be still very small. However, the efficiency of the energy transfer is much lower than 100 per cent, therefore we conclude that – at least in our 1D code – the turbulent convection has a negligible effect in altering the light-curve shape from cycle to cycle, although it provides the necessary viscosity to control the amplitude. We note in passing that Buchler, Kolláth & Cadmus (2004) found a much more significant turbulent energy in RV Tauri models.

A logical step in this direction would be the use of multidimension hydrocodes, such as Mundprecht, Muthsam & Kupka (2013), that would naturally enable the enhancement of turbulent energy or turbulent flux locally (see their fig. 12) as opposed to the zone-averaged quantities in our 1D simulations. However, given the large difference we found between the kinetic and turbulent energies, it is

highly questionable whether the required drastic change can occur in these overtone Cepheid models.

### 5.3 Period change

Several causes have been suggested for period variations in Cepheids, both fundamental mode pulsators and overtone pulsators.

(i) *Evolution* through the instability strip: this is almost certainly responsible for some of the period changes seen. While evolution does not necessarily proceed at a uniform pace (Fernie, Kamper & Seager 1993), one direction of period change would predominate and result in a parabolic O – C diagram.

(ii) *Light-time effects* in binary systems: this produces cyclic apparent period changes. They must, however, be consistent with what is known about the orbit of the system. Possibly the best example is AW Per (Welch & Evans 1989). Light-time effect has been suggested to explain the O – C residuals in RT Aur (Turner et al. 2007). However, the velocity variations shown in Fig. 9 indicate no variation larger than  $\pm 1 \text{ km s}^{-1}$  of the mean. This implies that an orbital velocity variation has not been observed for data drawn from many different instruments over a long time interval.

As discussed above, a substantial fraction (24 per cent) of overtone pulsators have period variations characterized by alternate (though cyclic) increases and decreases.

Light-time effect is the *one* explanation for period change which is cyclic, but it is not viable for many of the overtone pulsators because of the scale and erratic nature. This implies that these quasi-cyclic period variations are caused by something in the pulsation process itself.

(iii) *Star spots*: Neilson & Ignace (2014) have suggested that the period variations of the *Kepler* Cepheid V1154 Cyg could be produced by a hotspot on the surface caused by convection. In a study of yellow supergiants including several Cepheids, Percy & Kim (2014) suggest a similar possible cause for amplitude variation, large convection cells causing variation as the star rotates. While starspots could affect the time of maximum light, they would not have a cumulative effect as seen in the O – C diagram.

(iv) *Mass-loss*: this has been suggested, for instance by Neilson, Cantiello & Langer (2011) and Neilson et al. (2012), and worked out in detail. However, since periods change *monotonically*, the quasi-cyclic variations frequently seen in overtone pulsators are not due to mass-loss. We note, however, that the period changes in overtone pulsators discussed in Section 5 which can reasonably be fitted with parabolas all show increasing periods. This is consistent with mass-loss, although it may be only one of several factors.

(v) *Pulsation*: amplitude variation in Blazhko RR Lyr stars is not fully understood, but one possible explanation is that it is produced by high-order resonance (Buchler & Kolláth 2011). Pulsation and excitation of a complicated group of modes may also play a role in Cepheid period change. Percy & Kim (2014) suggest that convection may drive pulsation mode excitation and hence amplitude variation, and the same might also affect Cepheid periods. As discussed above, the fact that the level of pulsation instability on both short and long time-scales appears to depend on pulsation mode suggests a role for pulsation in period changes.

The observed period changes may be due to a combination of these factors. However, the morphology of O – C diagrams, particularly for overtone pulsators, provides some clues. In particular, the high fraction of overtone pulsators which have quasi-cyclic period variations is not consistent with stellar evolution nor mass-loss. Furthermore, the size of the variations is too large to uniquely originate

from binary light-time effects. Hence the pulsation process itself is indicated as a cause.

## 6 CONCLUSIONS

There are three primary results from the *MOST* observations of Cepheids.

(i) The observations of a fundamental mode pulsator (RT Aur) and an overtone pulsator (SZ Tau) find greater instability in the pulsation of the overtone Cepheid in the repetition of the light curve and the Fourier parameters.

(ii) On the other hand, the deviations between cycles for both RT Aur and SZ Tau follow a similar pattern as a function of phase of increase after minimum radius and a return to a smaller value after maximum radius.

(iii) The O – C curves indicate that on a time-scale of decades, the period changes of the overtone pulsator are more erratic.

Thus at both long and short time-scales, the period variations of RT Aur (fundamental mode) and SZ Tau (overtone mode) differ, with the overtone mode pulsator exhibiting greater instability at all time-scales.

## ACKNOWLEDGEMENTS

We are happy to thank Joseph E. Postma for his unpublished photometric data. We also thank Zoltán Kolláth for enlightening discussions. Comments from an anonymous referee have improved the text, particularly in Section 4. This project has been supported by the ‘Lendület-2009 Young Researchers’ Program of the Hungarian Academy of Sciences, and the Hungarian OTKA grant K83790. The research leading to these results has received funding from the European Community’s Seventh Framework Programme (FP7/2007-2013) under grant agreement no. 269194 (IRSES/ASK) and no. 312844 (SPACEINN). Funding has also been received from the ESA PECS Contract No. 4000110889/14/NL/NDe. RS and AD were supported by the János Bolyai Research Scholarship of the Hungarian Academy of Sciences. RS thanks the hospitality of CfA during a visit. Financial support for LS was provided from the ESTEC Contract No.4000106398/12/NL/KML. Support for this work was also provided from the Chandra X-ray Center NASA Contract NAS8-03060 (for NRE). JMM, DBG, AFJM and SMR are grateful for financial aid from NSERC (Canada) and AFJM also to FRQNT (Quebec). WWW was supported by the Austrian Science Fonds (FWF P22691-N16) This research has made use of the SIMBAD data base, operated at CDS, Strasbourg, France.

## REFERENCES

- Arellano Ferro A., 1983, ApJ, 274, 755
- Arellano Ferro A., Rojo Arellano E., Gonzalez-Bedolla S., Rosenzweig P., 1998, ApJS, 117, 167
- Barnes T. G., III, Moffett T. J., Slovak M. H., 1987, ApJS, 65, 307
- Barnes T. G., III Fernley J. A., Frueh M. L., Navas J. G., Moffett T. J., Skillen I., 1997, PASP, 109, 645
- Beavers W. I., Eitter J. J., 1986, ApJS, 62, 147
- Benedict G. F. et al., 2007, AJ, 133, 1810
- Berdnikov L. N., 2008, VizieR On-line Data Catalog: II/285
- Berdnikov L. N., Pastukhova E. N., 1995, Astron. Lett., 21, 369
- Berdnikov L. N., Ignatova V. V., Pastukhova E. N., Turner D. G., 1997, Astron. Lett., 23, 177
- Berdnikov L., Mattei J. A., Beck S. J., 2003, J. Am. Assoc. Var. Star Obs., 31, 146

- Bersier D., Burki G., Burnet M., 1994, *A&AS*, 108, 9  
 Bruntt H. et al., 2008, *ApJ*, 683, 433  
 Buchler J. R., Kolláth Z., 2011, *ApJ*, 731, 24  
 Buchler J. R., Kolláth Z., Cadmus R. R., 2004, *ApJ*, 613, 532  
 Burki G., Schmidt E. G., Arellano Ferro A., Fernie J. D., Sasselov D., Simon N. R., Percy J. R., Szabados L., 1986, *A&A*, 168, 139  
 Derekas A. et al., 2012, *MNRAS*, 425, 1312  
 Eggen O. J., 1951, *ApJ*, 113, 367  
 Evans N. R., 1976, *ApJS*, 32, 399  
 Evans N. R., 2000, *AJ*, 119, 3050  
 Evans N. R., Sasselov D. D., Short C. I., 2002, *ApJ*, 567, 1121  
 Feltz K. A., Jr McNamara D. H., 1980, *PASP*, 92, 609  
 Fernie J. D., 1993, *Inf. Bull. Var. Stars*, 3854, 1  
 Fernie J. D., Kamper K. W., Seager S., 1993, *AJ*, 416, 820  
 Gieren W. P., 1985, *A&A*, 148, 138  
 Gorynya N. A., Samus N. N., Rastorguev A. S., Sachkov M. E., 1996, *Astron. Lett.*, 22, 175  
 Groenewegen M. A. T., Oudmaijer R. D., 2000, *A&A*, 356, 849  
 Kienzle F., Moskalik P., Bersier D., Pont F., 1999, *A&A*, 341, 818  
 Kiess C. C., 1917, *Publ. Astron. Obs. Univ. Michigan*, 3, 131  
 Kiss L. L., 1998, *J. Astron. Data*, 4, 1  
 Koen C., 2006, *MNRAS*, 365, 489  
 Kolláth Z., Buchler J. R., Szabó R., Csabry Z., 2002, *A&A*, 385, 932  
 Lenz P., Breger M., 2005, *Commun. Asteroseismol.*, 146, 53  
 Matthews J. M., Kuschnig R., Guenther D. B., Walker G. A. H., Moffat A. F. J., Rucinski S. M., Sasselov D., Weiss W. W., 2004, *Nature*, 430, 51  
 Meyer R., 2004, *BAV Rundbrief*, 53, 37  
 Milone E. F., 1970, *Inf. Bull. Var. Stars*, 482, 1  
 Mitchell R. I., Iriarte B., Steinmetz D., Johnson H. L., 1964, *Bol. Obs. Tonantzintla y Tacubaya*, 3, 24  
 Moffett T. J., Barnes T. G., III 1984, *ApJS*, 55, 389  
 Molnar L., Szabados L., 2014, *MNRAS* 442, 3222  
 Mundprecht E., Muthsam H. J., Kupka F., 2013, *MNRAS*, 435, 3191  
 Neilson H. R., Ignace R., 2014, *A&A*, 563, L4  
 Neilson H. R., Cantiello M., Langer N., 2011, *A&A*, 529, L9  
 Neilson H., Engle S. G., Guinan E., Langer N., Wasatonic R. P., Williams D. B., 2012, *ApJ*, 745, 32  
 Peña J. H. et al., 2010, *Rev. Mex. Astron. Astrofis.*, 46, 291  
 Percy J. R., Kim R. Y. H., 2014, *J. Am. Assoc. Var. Star Obs.*, 42, 1  
 Petrie R. M., 1932, *Publ. Astron. Obs. Univ. Michigan*, 5, 3  
 Postma J. E., 2007, MSc thesis, Univ. of Calgary  
 Rowe J. F. et al., 2006a, *Mem. Soc. Astron. Ital.*, 77, 282  
 Rowe J. F. et al., 2006b, *ApJ*, 646, 1241  
 Sachkov M. E., 1997, *Inf. Bull. Var. Stars*, 4522, 1  
 Simon N. R., Teays T. J., 1982, *ApJ*, 261, 586  
 Sterken C., Jäschek C. eds 1996, *Light Curves of Variable Stars, A Pictorial Atlas*. Cambridge Univ. Press, Cambridge  
 Szabados L., 1977, *Mitt. Sternw. ung. Akad. Wiss.*, Budapest, No. 70  
 Szabados L., 1983, *Ap&SS*, 96, 185  
 Szabados L., 1991, *Commun. Konkoly Obs.*, No. 96  
 Szabó R., Buchler J. R., Bartee J., 2007, *ApJ*, 667, 1150  
 Szabó R. et al., 2010, *MNRAS*, 409, 1244  
 Takeda Y., Kang D. I., Han I., Lee B. C., Kim K. M., 2013, *MNRAS*, 432, 769  
 Turner D. G. et al., 2007, *PASP*, 119, 1247  
 Walker G. et al., 2003, *PASP*, 115, 1023  
 Walraven Th., Muller A. B., Oosterhoff P. Th., 1958, *BAN*, 14, 81  
 Wamsteker W., 1972, *Inf. Bull. Var. Stars*, 690, 1  
 Welch D. L., Evans N. R., 1989, *AJ*, 97, 1153  
 Williams J. A., 1966, *AJ*, 71, 615  
 Wilson T. D., Carter M. W., Barnes T. G., III, van Citters G. W., Jr, Moffett T. J., 1989, *ApJS*, 69, 951  
 Wisniewski W. Z., Johnson H. L., 1968, *Commun. Lunar Planet. Lab.*, 7, 112

## SUPPORTING INFORMATION

Additional Supporting Information may be found in the online version of this article:

**Table 3.** *O – C* values of RT Aurigae. *E* is the epoch of the determination in cycles; *W* is the weight.

**Table 5.** *O – C* values of SZ Tauri.

**Table 6.** New *UBV* photometric data of SZ Tauri. (<http://mnras.oxfordjournals.org/lookup/suppl/doi:10.1093/mnras/stu2371/-/DC1>).

Please note: Oxford University Press are not responsible for the content or functionality of any supporting materials supplied by the authors. Any queries (other than missing material) should be directed to the corresponding author for the article.

This paper has been typeset from a  $\text{\TeX}/\text{\LaTeX}$  file prepared by the author.